Synchronic integration of ultrasound radiation and ZnO nanoparticles for biodiesel generation: Optimization by central composite design

Abstract

This study investigated the enhancement of biodiesel yield produced from sunflower oil via the transesterification process using a zinc oxide (ZnO) nanocatalyst under ultrasonic irradiation. The properties of the nanocatalyst prepared by the sol-gel method were characterized by XRD, FTIR, SEM, and TEM analyses. The ZnO nanoparticles had an average size of 24 nm with a hexagonal, slightly spherical structure. Response Surface Methodology (RSM) and Central Composite Design (CCD) were applied to evaluate the effect of influential parameters on methyl ester yield. Besides, the accuracy of the suggested model was confirmed by Analysis of Variance (ANOVA). A reasonable accordance between the experimental and predicted data was achieved with $R^2 = 0.9968$ and adjusted $R^2 = 0.9938$. The optimum process conditions were a methanol/sunflower oil molar ratio of 10.98 mol/mol, an ultrasonic time of 26.28 min, and a nanocatalyst loading of 2.71 wt.%. Under these conditions, the RSM model predicted a maximum biodiesel yield of 90.5%, while the highest experimental yield obtained was 89.57%, confirming the accuracy of the model. Moreover, FTIR analysis of the produced biodiesel confirms successful synthesis. The nanocatalyst demonstrated high reusability over seven cycles, maintaining a biodiesel yield above 80% after the seventh use, indicating excellent recyclability. Therefore, this research demonstrated that the combination of ultrasonic radiation and ZnO particles presents a promising approach for biodiesel production, enabling high efficiency within a short reaction time.

Keywords: Biodiesel, Transesterification, Nanocatalyst, Zinc Oxide, Ultrasonic radiation, Response Surface Methodology

1. Introduction

Non-renewable energies have been a significant source of fuel for domestic and industrial uses for several decades. However, these non-renewable fuels, whose reserves and production are limited and take years to replenish, are not sustainable energy sources [1]. Extensive use of petroleum products in recent decades has caused fuel shortages, environmental pollution, and numerous health crises for humans [2]. Due to drawbacks such as the depletion of fossil fuel resources and associated environmental limitations, biofuels have gained global attention as a clean, sustainable, and renewable alternative [3, 4]. In this context, biofuels are considered a significant priority because of their sustainability, renewability, and cleaner nature. Diesel fuels have been an important fuel source in the past decade, making the development of efficient biofuels with properties similar to diesel fuels crucial. One of the most suitable fuels to replace diesel is biodiesel, a sustainable fuel capable of saving the environment [5, 6]. Biodiesel possesses properties similar to conventional diesel fuel, making it usable in various applications [7, 8]. Biodiesel contains a high oxygen content, which promotes more complete combustion and consequently reduces greenhouse gas emissions [9, 10]. Traditionally, it has been produced from first-generation edible vegetable oils such as palm, rapeseed, soybean, and sunflower oils [11]. However, the extensive use of edible oils raises concerns regarding food security, land use, and high production costs, leading to the well-known 'food versus fuel' debate. To address these issues, researchers have increasingly turned to non-edible and alternative feedstocks, including palm kernel oil, castor oil, jatropha, waste cooking oils, animal fats, and algal biomass, which offer a more sustainable and economically viable pathway for biodiesel production [12,13].

Biodiesel is most often synthesized through the transesterification process, where the performance of the catalyst determines both yield and efficiency. Unlike homogeneous systems, heterogeneous catalysts remain in the solid phase, while methanol and the oil feedstock exist in the liquid phase. This difference between phases provides a major advantage, as the catalyst can be recovered by straightforward operations such as filtration, centrifugation, or sedimentation [14, 15]. The simplicity of recovery reduces downstream processing steps, lowers purification costs, and makes biodiesel production more cost-effective [16]. Beyond economic benefits, heterogeneous catalysts contribute to greener processing by limiting chemical waste and reducing environmental burdens.

Their activity originates from the adsorption of reactants onto the catalyst surface, where acidic functional sites provide positive charges and basic sites offer negative charges, enabling both transesterification and esterification reactions [17, 18]. In transesterification, alcohol molecules react with triglycerides to form an unstable tetrahedral structure that rearranges to generate esters while progressively releasing diglycerides and eventually glycerol. In esterification, alcohols act as nucleophiles, attacking carbonyl groups to form a similar intermediate that subsequently eliminates water or glycerol, resulting in ester production [19]. These reaction pathways highlight the ability of heterogeneous catalysts to deliver biodiesel efficiently while reducing both cost and environmental impact. Using heterogeneous catalysts offers an eco-friendly and cost-effective alternative to improve biodiesel yield and reduce reaction time. They also perform effectively with higher molecular weight alcohols. Basic heterogeneous catalysts are widely preferred over acidic ones due to their higher conversion rates and moderate reaction conditions [20]. Additional processing steps required for biodiesel production are minimized when using heterogeneous catalysts. These catalysts are easily recoverable and can be reused multiple times, which significantly lowers the overall commercial production cost of biodiesel [21, 22]. Although

heterogeneous catalysts offer notable benefits, they are often constrained by certain drawbacks, such as limited active site availability, restricted diffusion of reactants, reduced catalytic efficiency, and significant mass transfer resistance arising from the multiphase nature of the reaction system. An ideal heterogeneous catalyst should be highly efficient, stable, cost-effective, environmentally friendly, and porous. It must have a significant surface area, uniformly distributed pores of standard size, and long durability to replace homogeneous catalysts [23, 24]. Importantly, the catalytic activity is influenced by the catalyst's reactivity in ambient conditions, especially when stored in open air [25]. Transesterification is the primary process for biodiesel production, where triglycerides react with alcohol, catalyzed by heterogeneous catalysts, to form methyl esters. Since triglycerides and alcohol are immiscible liquids, the reaction occurs only at the phase interface, requiring prolonged mechanical mixing. The application of ultrasonic waves addresses this limitation effectively [26]. Ultrasound induces cavitation formation and collapse of microbubbles, creating a stable emulsion between phases, significantly increasing interfacial contact and mass transfer. This accelerates the reaction, reduces process time, and improves yield. Beyond providing mechanical mixing energy, ultrasound supplies the activation energy necessary to initiate the transesterification process [27, 28]. Numerous studies confirm that ultrasonic-assisted transesterification efficiently converts vegetable oils, waste oils, and animal fats into biodiesel, saving energy and producing higher purity products compared to conventional stirring methods. For instance, Maleki et al. [29] demonstrated that an α-Fe_2O_3/ZnO nanocatalyst used with canola oil under optimized ultrasonic conditions 22.29 min of irradiation, 278.46 W power, a methanol/oil molar proportion of 11.25:1, and 3 wt.% catalyst loading achieved a biodiesel yield of 94.21%. Notably, the purity of the biodiesel produced under ultrasonic assistance was approximately 40% higher than that obtained through conventional mechanical stirring.

This study assessed the effectiveness of ZnO nanoparticles as a heterogeneous catalyst under ultrasonic radiation for enhancing biodiesel production from sunflower oil. The ZnO nanocatalyst was prepared using the sol-gel technique and characterized in terms of crystal structure, morphology, functional groups, and particle size using XRD, SEM, and TEM analyses. Besides, the influence of critical reaction parameters, including the methanol/oil molar proportion, duration of ultrasonic irradiation, and ZnO nanoparticle loading, on biodiesel yield was examined. Statistical evaluation using Response Surface Methodology based on Central Composite Design was conducted to establish relationships between operational parameters and reaction performance. Furthermore, the recyclability of the ZnO nanocatalyst was studied across seven consecutive cycles under optimal conditions, demonstrating high catalyst stability.

2. Materials and Laboratory Equipment

2.1 Chemicals and oil used

Methanol (99.98%) was purchased from Merck, Germany, with a purity of 99.8%, and used as one of the three components in the transesterification reaction. Additionally, zinc acetate dihydrate ($Zn(CH_3COO)_2 \cdot 2H_2O$) was obtained as the precursor for zinc oxide synthesis. Sodium hydroxide (NaOH) and ethanol (C_2H_6O) were employed, respectively, as the precipitating agent and washing solvent for the nanocatalyst. Deionized water was also used as a washing agent.

Moreover, sunflower oil obtained from oil extraction (Esfarayen, Iran) was used in this study. The oil used in this study exhibited a density of 0.917 g/cm³ at 15 °C and a kinematic viscosity of 29.51 mm²/s at 40 °C, reflecting its moderate fluidity suitable for biodiesel synthesis. Its saponification value was measured at 195.3 mg KOH/g, indicating a typical triglyceride content, while the low acid value of 0.11 mg KOH/g suggested minimal free fatty acids, which is favorable

for transesterification reactions. The oil's calorific value was 39.42 MJ/kg, and the average molecular weight was calculated as 862.7 g/mol. Fatty acid analysis revealed that linoleic acid (C18:2) was the predominant component at 62.27 wt.%, followed by oleic acid (C18:1) at 20.63 wt.%. Palmitic (C16:0) and linolenic (C18:3) acids were present at 8.56 wt.% and 5.12 wt.%, respectively, while stearic acid (C18:0) accounted for 3.42 wt.%. The high proportion of polyunsaturated fatty acids, combined with low free fatty acid content, indicates that this sunflower oil is highly suitable as a feedstock for biodiesel production, providing both good reactivity and efficient conversion under transesterification conditions.

The operational devices employed in this research included a magnetic stirrer model made in Germany, an Agilent gas chromatography device model 6890N manufactured in Switzerland, a centrifuge model Centric 150 Domel, an ultrasonic homogenizer model Bandelin Sono-puls hd 2200 made in Iran, and a digital balance with an accuracy of 0.001 g, model LABEX INSTRUMENT, manufactured in the United Kingdom.

2.2 Experimental design using response surface methodology

In this study, Design Expert software was employed to optimize the transesterification parameters, including the molar proportion of methanol/sunflower, nano-catalyst concentration, and ultrasonic irradiation time, in relation to biodiesel yield. The effects of three independent variables at five levels were investigated using the RSM-CCD method, comprising 20 experiments. It is noteworthy that the reaction temperature was kept constant at 65 °C in all experiments. Furthermore, a second-order polynomial model, derived from Eq. 1, was employed to describe and predict the relationship between the effective variables and the response, specifically the biodiesel yield (BY) [28, 30].

$$BY = b_0 + \sum_{i=1}^{k} b_i X_i + \sum_{i-1}^{k} b_{ii} X_i^2 + \sum_{i=1}^{k} \sum_{j=i+1}^{k} b_{ij} X_i X_j + \varepsilon \quad (1)$$

Here, X_i and X_j represent operational parameters (e.g., the molar proportion of methanol to sunflower oil, ultrasonic time, and concentration of zinc oxide nano-catalyst). Besides, b_0 and ε denote the intercept and random error, respectively. The coefficients b_i, b_{ii}, and b_i are model constants extracted from statistical analysis [31]. Table 1 presents the experimental ranges and levels of the three key parameters used in this research for designing the experiments and achieving the highest biodiesel yield from sunflower oil via transesterification.

Table 1. Variation range and values of the three critical factors used in this study

No.	Variables	Notation	-2	-1	0	+1	+2
1	Molar Ratio (mol: mol)	X_1	6.64	8	10	12	13.36
2	Ultrasonic Time (min)	X_2	14.89	20	27.5	35	40.11
3	Catalyst Content (wt.%)	X_3	1.32	2	3	4	4.68

2.3 Preparation of ZnO nanocatalyst

Zinc oxide nanoparticles were prepared via the sol-gel approach [29]. Initially, a 1 M solution of zinc acetate dihydrate was made by dissolving the calculated amount in methanol and stirring magnetically at 70 °C for 2 h. Then, 1 M NaOH was added gradually until the mixture turned milky and the pH reached around 10. Following precipitation, the suspension was stirred at ambient temperature for 1 h. The solid product was separated by centrifugation at 5000 rpm for 15 min, dried in an oven at 120°C for 3 h, and then calcined at 550 °C for 2 h to obtain ZnO nanocatalysts. The structural and morphological properties of the synthesized ZnO nanoparticles were examined using FTIR (Thermo Scientific, Nicolet iS50) to identify functional groups, SEM (Hitachi,

SU3500) for surface morphology, XRD (Bruker, D8 Advance) for crystalline structure, and TEM (FEI, Tecnai G_2) to determine particle size.

2.4 Ultrasonic-Assisted Transesterification Reaction

A mixture of sunflower oil, methanol, and ZnO nanocatalyst was introduced into a sono-reactor to start the transesterification reaction. The ultrasonic amplitude was controlled via a controller and kept constant at 50% throughout all experiments. Using an RSM-CCD approach, the effects of methanol/oil proportion, catalyst loading, and ultrasonic irradiation time on biodiesel production from sunflower oil were evaluated. Based on the experimental design, the post-reaction mixture was separated in a Buchner funnel into glycerol (bottom layer) and biodiesel (top layer). Subsequent purification steps included glycerol isolation to obtain a clear methyl ester [32, 33]. Figure 1 provides a schematic illustration of biodiesel generation from sunflower oil utilizing ZnO nanoparticles under ultrasonic irradiation.

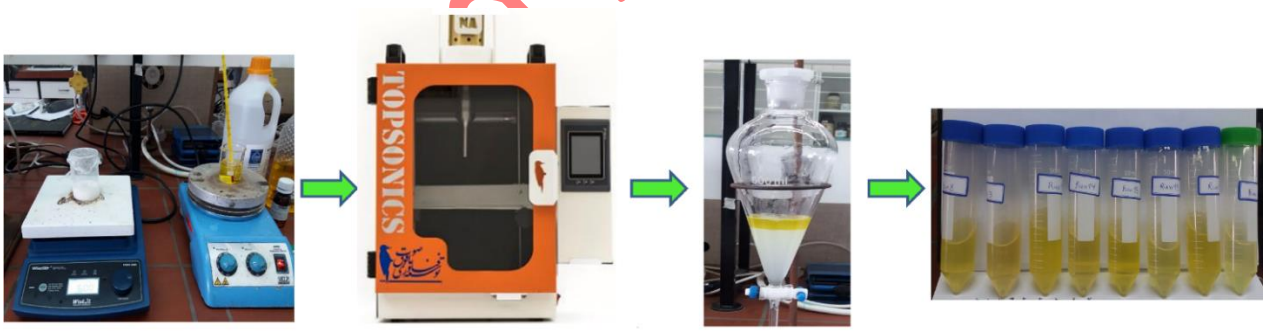

Figure 1. Various stages of biodiesel production, separation, and purification.

In the biodiesel purification stage, a heating process was applied to remove residual substances such as methanol and moisture. The produced biodiesel was placed in an oven at 100 °C for 80 min to evaporate the remaining methanol and moisture. The resulting clear biodiesel was then sent

to Bim Gostar Taban laboratory for gas chromatography mass spectrometry (GC-MS) testing. Finally, the biodiesel yield was calculated using equation (2) [29, 34].

$$\text{Biodiesel yield } (\%) = \frac{mass\ of\ biodiesel\ generated(g)}{mass\ of\ oil\ (g)} \times 100 \qquad (2)$$

3. Results and Discussion

3.1 Characterization of zinc oxide nanocatalyst

3.1.1 XRD analysis

The XRD patterns of the fabricated zinc oxide are shown in Figure 2. The XRD results indicate that the ZnO nanoparticles exhibited intense peaks that perfectly match JCPDS: 36-451 for zinc oxide nanoparticles. Furthermore, Figure 2 confirms that no impurities exist in the synthesized nanocatalyst [8]. Moreover, the 2θ values at approximately 33.21°, 36.47°, 38.71°, 49.68°, 58.89°, 66.83°, 69.97°, 74.28°, and 76.22° correspond respectively to the reflection planes (101), (002), (100), (102), (110), (103), (200), (112), and (201) [35].

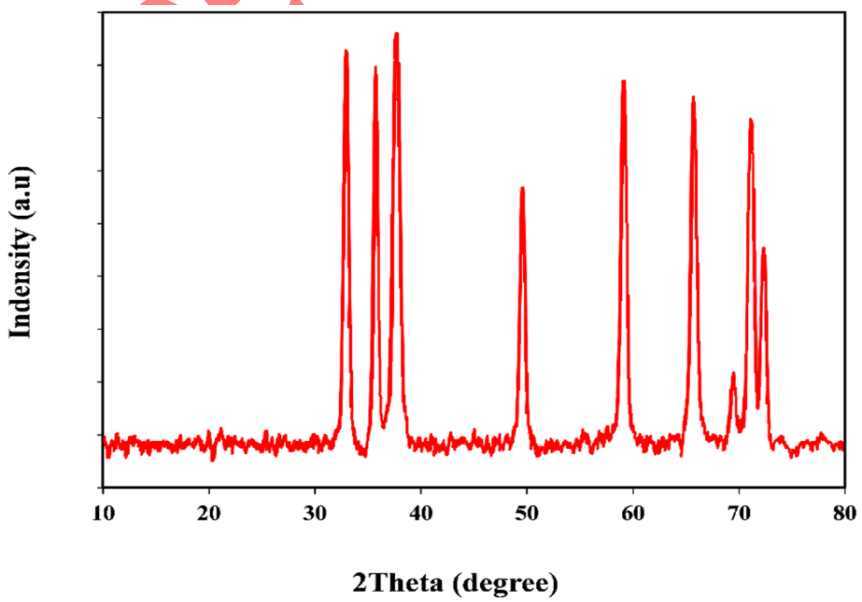

Figure 2. XRD analysis of zinc oxide nanocatalyst prepared using the sol-gel approach.

3.1.2 FTIR analysis

The FTIR spectrum of the zinc oxide nanocatalyst in the 400–4000 cm^{-1} range is presented in Figure 3. A strong peak around 432 cm^{-1} is attributed to the Zn–O stretching vibration, confirming the formation of the zinc oxide structure. A characteristic peak at 3443 cm^{-1} corresponds to the O–H stretching vibration, indicating hydroxyl groups on the nanoparticle surface. These groups play an important role in enhancing hydrophilicity and providing active catalytic sites. Absorption peaks at 1383, 1514, and 1628 cm^{-1} relate to symmetric and asymmetric bending vibrations of C=O groups, showing the presence of carbonyl functional groups [34, 35]. A relative intensity decrease in the 2500–2700 cm^{-1} region corresponds to weak vibrational absorption. Additionally, smaller peaks at 936 and 1139 cm^{-1} are due to Zn–O metal-oxygen vibrations, further confirming the distinctive crystalline structure of ZnO.

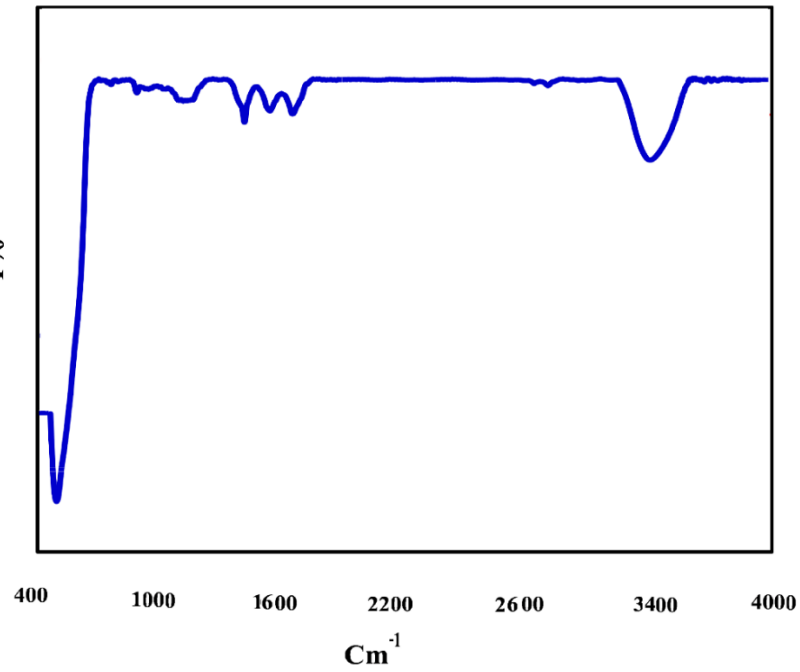

Figure 3. FTIR pattern of the synthesized zinc oxide nanocatalyst.

3.1.3 Morphological analysis (SEM/TEM)

The morphology and surface characteristics of the synthesized zinc oxide nanocatalysts were investigated using SEM and TEM analyses. As shown in Figure 4(a), numerous fine particles are present within the catalyst structure, some of which form aggregated and interconnected clusters. Additionally, petal-like structures are discernible on the surface morphology of the nanocatalyst. The presence of a large specific surface area and numerous active pores in these structures is essential for boosting transesterification efficiency. Besides increasing the contact surface, these flower-like morphologies improve the penetration of alcohol and oil into the active catalytic sites.

TEM images in Figure 4(b) complement the SEM results, revealing that the zinc oxide particles mostly form near-spherical hexagonal shapes with sizes less than 50 nm. Such nanometric dimensions and regular morphology, due to the high surface-to-volume ratio and numerous active centers, lead to increased reactivity and improved catalytic performance in biodiesel synthesis.

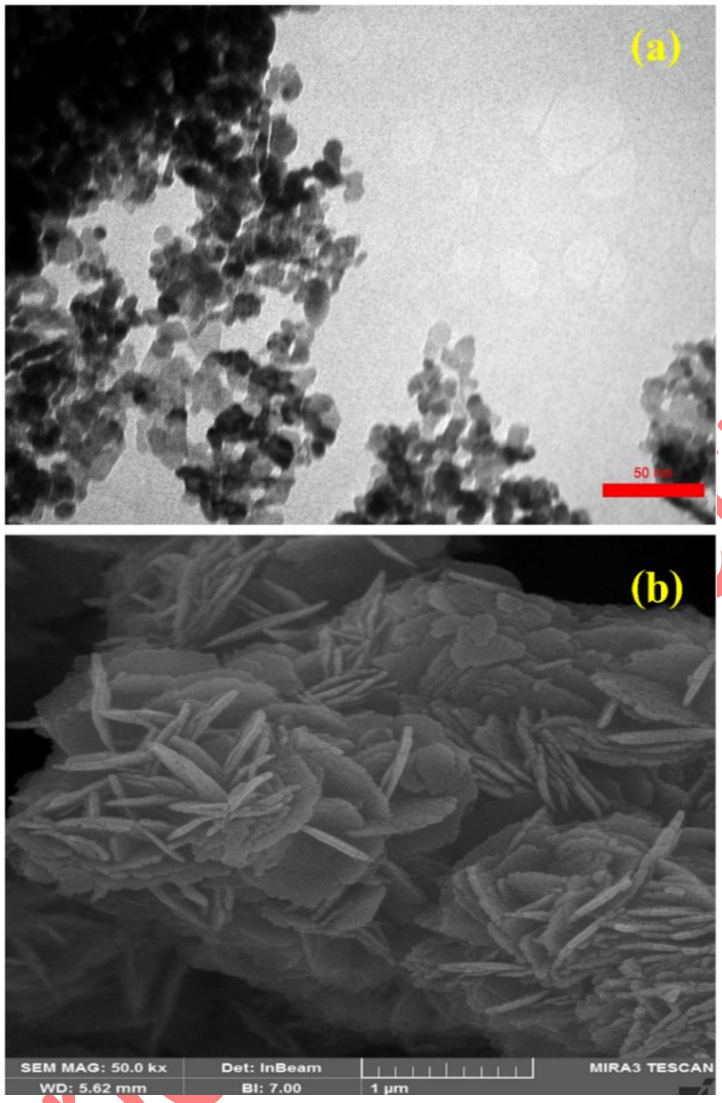

Figure 4. Morphological analysis of ZnO nanoparticles: TEM image (a) and SEM image (b).

3.2 Model Validation Using RSM-CCD

Based on the selected parameters, the experimental values of biodiesel yield derived from sunflower oil are presented in Table 2. According to this table, significant variations in biodiesel yield are observed at different amounts of the chosen factors. These results indicate that the selection and range of transesterification parameters in the experimental design were appropriately determined.

Table 2. Experimental matrix of CCD with corresponding biodiesel production results.

	Factors			Response
No.	Methanol/oil (mol: mol)	Ultrasonic time (min)	Catalyst loading (wt.%)	Yield (%)
1	13.36	27.50	3.00	77.64
2	8.00	35.00	2.00	62.24
3	6.64	27.50	3.00	58.22
4	8.00	20.00	4.00	70.39
5	10.00	27.50	3.00	89.57
6	12.00	35.00	4.00	63.13
7	10.00	27.50	3.00	89.57
8	10.00	40.11	3.00	69.72
9	10.00	27.50	3.00	88.65
10	12.00	20.00	4.00	72.64
11	10.00	27.50	3.00	89.57
12	10.00	27.50	3.00	88.73
13	8.00	35.00	4.00	62.48
14	12.00	20.00	2.00	80.81
15	12.00	35.00	2.00	79.82
16	10.00	14.89	3.00	75.36
17	10.00	27.50	1.32	67.43

18	10.00	27.50	4.68	64.65
19	10.00	27.50	3.00	88.42
20	8.00	20.00	2.00	56.32

RSM coupled with CCD was utilized to assess the impact of critical process variables on biodiesel production. This approach, recognized as an efficient experimental design tool, enables simultaneous investigation of both main and interaction effects of variables, offering high accuracy in process response prediction [36]. In this study, three main variables were selected: molar ratio of methanol/sunflower oil, nanocatalyst concentration, and ultrasound time. Their influence on biodiesel production efficiency was assessed, with results presented in Tables 2 and 3. Run 11 produced the highest biodiesel yield (89.57%) at optimal settings: methanol/oil proportion of 1:10, nanocatalyst loading of 3 wt.%, ultrasonic duration of 27.5 min, and temperature maintained at 65 °C. Statistical analysis confirmed that all variables and their interactions were highly significant (p-value < 0.05), demonstrating a notable impact on yield. The model fit quality was excellent, with R^2 and adjusted R^2 values exceeding 0.98. The F-values indicate the relative significance of the variables, revealing that the methanol-to-oil molar ratio (F = 529.68) was the most influential factor, followed by ultrasonic time (F = 42.44) and catalyst concentration (F = 20.37) [37, 38]. Regarding interactions, the ultrasonic time and methanol/oil ratio interaction had the lowest significance (F= 10.87), whereas the quadratic effect of ultrasonic time alone had the greatest influence (F= 1097.14) on improving yield. Model lack-of-fit error was negligible, and a low coefficient of variation (C.V= 1.22) confirmed high model precision [39]. Therefore, the selected second-order polynomial model is reliable for predicting biodiesel yield under various operational conditions. The final mathematical model for predicting biodiesel yield (%) is given as:

Yield (%) = +89.06 +5.68 A -1.61 B -1.11 C- 1.06 AB -4.90 AC -2.79 BC -7.30 A^2 -5.67 B^2-7.96 C^2 (3)

Table 3. ANOVA results from response surface method for biodiesel yield produced using ultrasonication.

Source	sum of squares	Degrees of freedom	average of squares	F-value	p-value
Model	2556.57	9	284.06	340.97	< 0.0001
Molar ratio (X_1)	441.28	1	441.28	529.68	< 0.0001
Ultrasonic time (X_2)	35.36	1	35.36	42.44	< 0.0001
Catalyst amount (X_3)	16.97	1	16.97	20.37	0.0011
X_1X_2	9.05	1	9.05	10.87	0.0081
X_1X_3	191.79	1	191.79	230.21	< 0.0001
X_2X_3	62.44	1	62.44	74.95	< 0.0001
X_1^2	767.09	1	767.09	920.76	< 0.0001
X_2^2	462.63	1	462.63	555.31	< 0.0001
X_3^2	914.03	1	914.03	1097.14	< 0.0001
Lack of fit	8.33	10	0.83	4.69	0.0577
R-Squared	0.9968	Adj R-Square	0.9938	C.V. %	1.22

3.3 Effect of independent reaction parameters on biodiesel yield

To investigate the factors affecting biodiesel yield, three key parameters were evaluated: nanocatalyst concentration, reaction time, and molar proportion of methanol to sunflower oil. Nanocatalyst concentration is one of the most critical variables because increasing it raises the number of active sites on the nanoparticle surface, thereby improving biodiesel yield. As shown in Figures 5(b,c), increasing the concentration of zinc oxide nanocatalyst initially increases the yield, followed by a decrease. At low concentrations, the limited number of active sites and inadequate pore distribution lead to low biodiesel production [17, 38]. Raising the catalyst concentration up to an optimal level enhances access to active sites and facilitates alkyl ester production, directly improving transesterification performance. However, concentrations beyond the optimum increase the mixture's viscosity and cause insufficient mixing between oil and methanol, which raises mass transfer resistance and reduces biodiesel yield.

Reaction time also significantly influences yield and process economy [27, 38]. As observed in Figures 5(a,c), increasing ultrasonic irradiation time initially raises biodiesel yield but subsequently causes a decline. At ultrasonication times beyond the optimal value, a gradual decline in biodiesel yield was observed. This decrease can be attributed to the partial poisoning of catalyst surface sites caused by the excessive adsorption of by-products such as glycerol and methyl esters, which restricts access to active catalytic centers [13, 27]. Additionally, prolonged sonication may increase the viscosity of the reaction medium and promote nanoparticle agglomeration, both of which hinder effective mass transfer and reduce catalytic activity [31]. As a result, biodiesel conversion decreases at extended reaction times despite initially favorable conditions. On the other hand, transesterification kinetics depend on cavitation bubble formation and collapse in the

reaction mixture; prolonged times reduce the reaction between methoxide ions and triglycerides, leading to equilibrium and lowering the final yield [39, 40].

The molar proportion of methanol/sunflower oil is another determining factor of biodiesel yield. Increasing this ratio from 10 to 12 enhances yield because methanol molecules react with fatty acids to produce methoxide ions, accelerating transesterification. Methoxide plays a vital role in breaking carbonyl bonds and producing methyl esters while increasing the reaction's kinetic energy [41]. However, excessive methanol ratios cause high methanol concentration on the nanocatalyst surface, reducing access to fatty acids, slowing the reaction rate, and decreasing biodiesel yield. Therefore, optimizing nanocatalyst concentration, ultrasonic irradiation time, and methanol/oil molar ratio is essential to achieve high biodiesel yields. Failure to maintain optimal conditions can reduce process efficiency [42]. These results highlight the fundamental importance of precise control over these parameters in the operational design of transesterification processes for producing high-quality biodiesel with maximum yield.

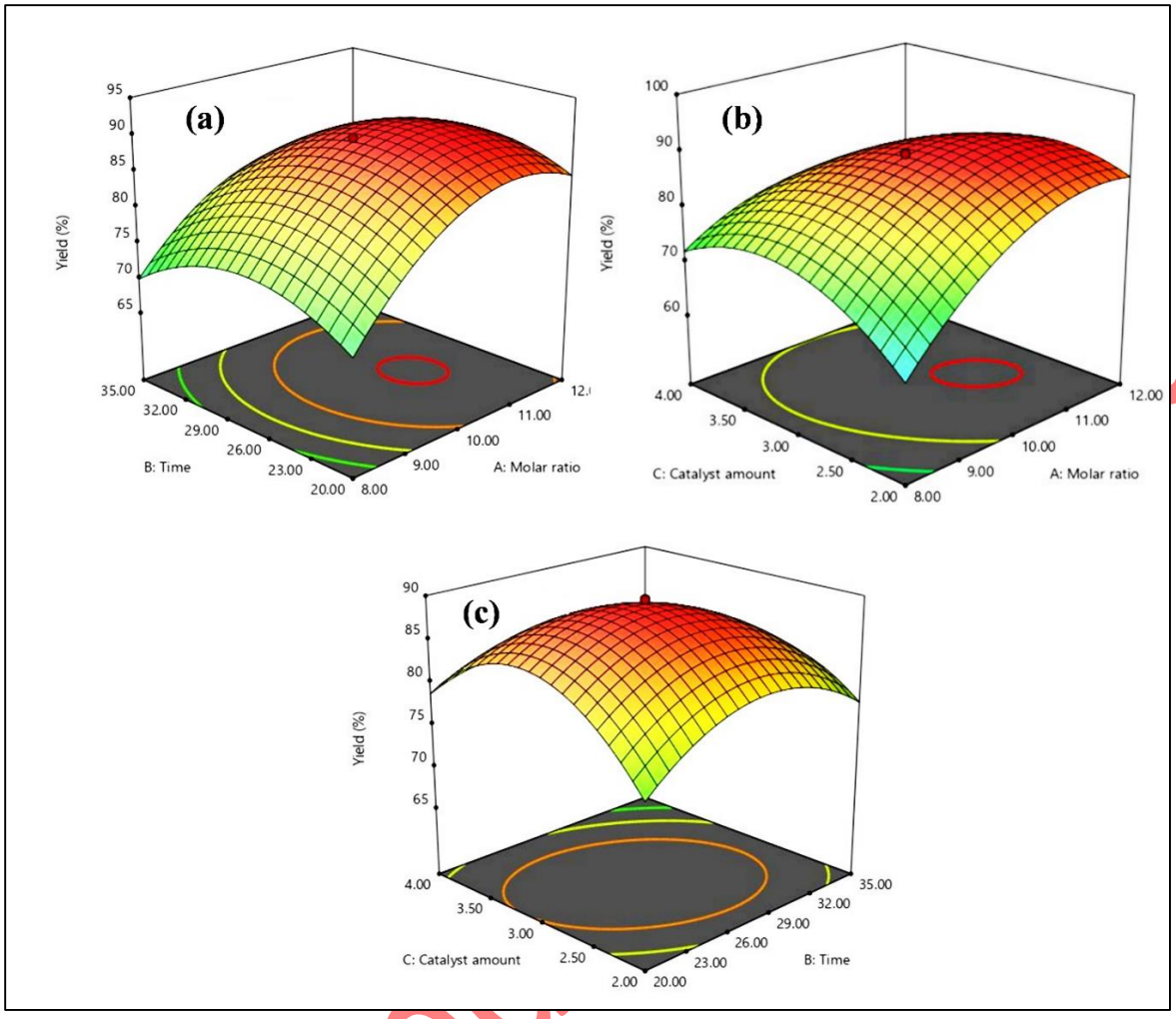

Figure 5 Response Surface and Interaction Plots (a) influence of methanol/oil ratio and sonication time, (b) influence of methanol/oil ratio and catalyst dosage, and (c) influence of sonication time and catalyst concentration on biodiesel yield.

3.4 Comparison of biodiesel production via ultrasonic and conventional methods

In this section, the transesterification process was examined to compare the efficiency of ultrasonic and conventional (magnetic stirring) methods under optimized conditions. The process was conducted using a methanol/oil proportion of 10.98:1, 2.71 wt.% ZnO nanoparticles, at 65 °C, with varying reaction times. Ultrasonic irradiation times ranged from 10 to 25 min, whereas for

magnetic stirring, much longer durations from 60 to 240 min were applied. Besides, the results shown in Figure 6 indicate that in the conventional method, biodiesel yield increased gradually and steadily with reaction time. However, the ultrasonic method achieved a significant increase in methyl ester yield even at shorter reaction times. This is attributed to cavitation bubbles formed in the reactor, which rapidly expand and violently collapse, providing the energy necessary for the reaction to occur efficiently [47]. The collapse generates vortices, acoustic streaming, and active radicals, while resulting microjets disrupt the interface between reactant phases, forming a stable emulsion [48]. This phenomenon increases the contact surface between oil and methanol and improves access to catalyst active sites, leading to a significant acceleration of the reaction rate and reduction of reaction time [47, 49]. Additionally, the ultrasonic method consumes less energy compared to magnetic stirring while enhancing biodiesel yield. It is noteworthy that in this study, the abbreviations MS and US refer to magnetic stirring and ultrasonic methods, respectively. These results highlight that ultrasonic energy application is an effective and green strategy to optimize the transesterification process and achieve high biodiesel yields.

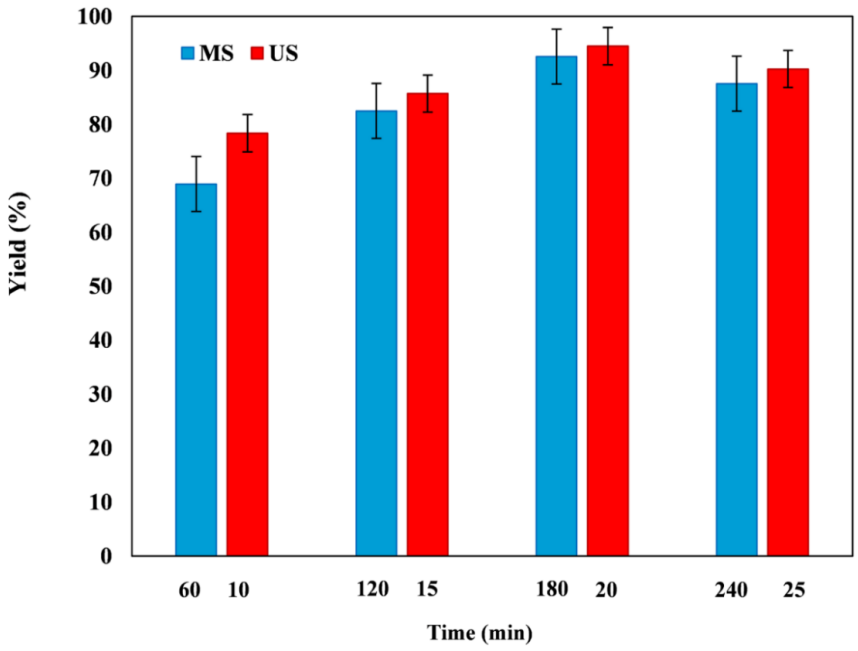

Figure 6. Comparison of the influence of the transesterification approaches on biodiesel yield.

3.5 Process Optimization

According to Figure 7, the maximum experimental biodiesel yield achieved using the zinc oxide nanocatalyst was 89.57%, demonstrating an acceptable yield for a pure metal oxide under mild operational conditions. The RSM-CCD model predicted a slightly higher optimum yield of 90.5% under the corresponding conditions. The optimal process parameters determined by the model were a methanol/oil molar ratio of 10.98, a nanocatalyst concentration of 2.71 wt.%, and an ultrasonication time of 26.28 min. Table 2 presents the experimental results for the zinc oxide nanocatalyst, showing that the maximum experimental biodiesel yield of 89.57% was obtained under conditions close to the predicted optimum (sonication time: 30 min, catalyst loading: 3 wt.%, methanol/oil ratio: 11). Consequently, the experimental findings are consistent with the predictions derived from RSM-CCD.

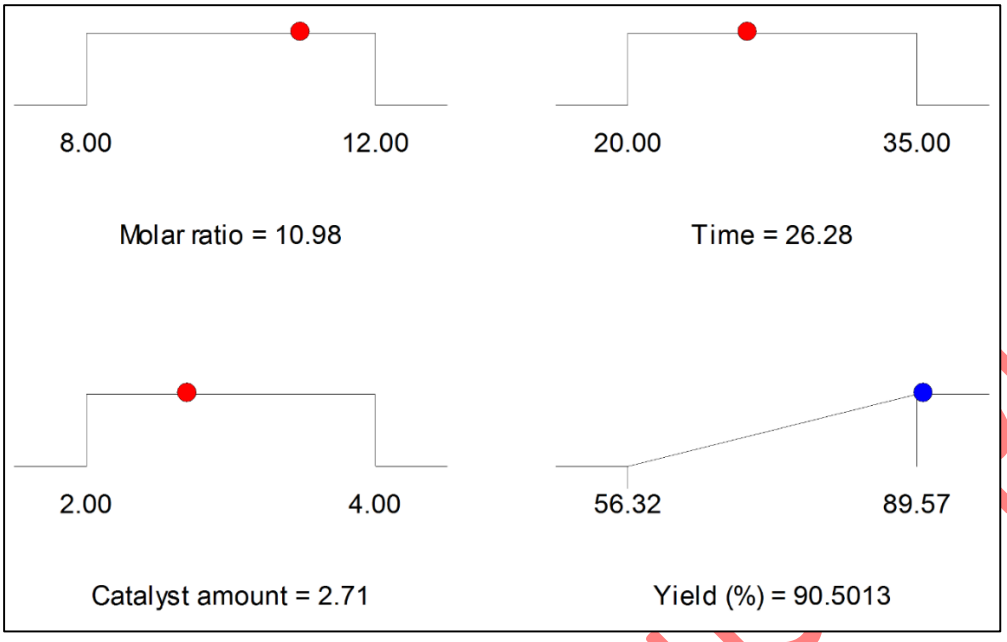

Figure 7. Optimized values of influential parameters by RSM-CCD.

3.6 Characterization of methyl ester

3.6.1 GC-MS analysis

The fatty acid content of biodiesel was characterized via GC–MS, with 1 µL of a sample (0.08 g methyl laurate, 5 mL hexane, 0.3 g biodiesel) injected at 280 °C (injector) and 300 °C (detector), using air and nitrogen flows of 400 and 45 mL/min, respectively. The results indicated that the dominant compounds in the biodiesel were methyl oleate and methyl linoleate with abundances of 20.13% and 61.34%, respectively. Other identified methyl esters included methyl palmitate (8.42%), methyl stearate (3.29%), and methyl linolenate (4.97%). Table 4 presents the fatty acid compositions of sunflower oil alongside the corresponding methyl esters produced in the biodiesel. These data demonstrate that triglycerides in the oil were converted into fatty acid methyl esters via ultrasound-assisted transesterification.

Table 4. Results of GC-MS analysis of sunflower oil components and corresponding derived biodiesel.

Fatty acid	Structure	TGs (wt.%)	FAMEs (wt.%)
Palmitic acid	C16:0	8.56	8.42
Stearic acid	C18:0	3.42	3.29
Oleic acid	C18:1	20.63	20.13
Linoleic acid	C18:2	62.27	61.34
Linolenic acid	C18:3	5.12	4.97

3.6.2 FTIR analysis of methyl ester

FTIR analysis was carried out to determine the functional groups in both sunflower oil and the biodiesel synthesized with ZnO nanocatalyst, as illustrated in Figure 8. Due to the chemical structural similarity between sunflower oil and the produced biodiesel, the intensity and peak range in both samples were nearly alike. In the sunflower oil spectrum, two main peaks at 2871 and 2902 cm^{-1} correspond to stretching vibrations of $–CH_3$ and $–CH_2$ groups [40]. Additionally, weak peaks at 761 and 3342 cm^{-1} were assigned to bending vibrations of $(CH_2)_n$ and hydroxyl groups (O–H), respectively. Other peaks at 623, 1080, 1382, and 1679 cm^{-1} were related to stretching vibrations of –C–H, $–OCH_3$, bending of $–CH_2$, and carbonyl (C=O) stretching bonds [39, 41]. After the transesterification reaction with ZnO nanocatalyst, changes in peak intensity and amplitude were limited, but slight shifts were observed. Peaks originally at 622, 761, 1080, 1382, 1731, and 2902–3302 cm^{-1} shifted to 615, 752, 1103, 1374, 1724, 2891, and 3389 cm^{-1}, respectively. These shifts

indicate minor chemical changes and confirm the conversion of sunflower oil into biodiesel [42]. The FTIR spectrum of the produced biodiesel demonstrated a strong and sharp absorption peak near 1724 cm^{-1}, attributed to the ester C=O stretching vibration, which confirms the formation of FAMEs [27]. Additionally, characteristic bands associated with $–OCH_3$ groups and C–O–C stretching appeared in the 1146 cm^{-1} region, further supporting successful transesterification. A peak at 946 cm^{-1} was also observed, assigned to out-of-plane =C–H bending/ C–O– stretching, consistent with the presence of alkyl ester functional groups. While this peak supports biodiesel formation, the primary confirmation arises from the strong carbonyl (C=O) and $–OCH_3$ bands, as noted above [38, 40]. Hence, these FTIR changes confirm that the zinc oxide nanocatalyst can effectively perform transesterification while preserving the overall structure of functional groups, resulting in high-purity, quality biodiesel.

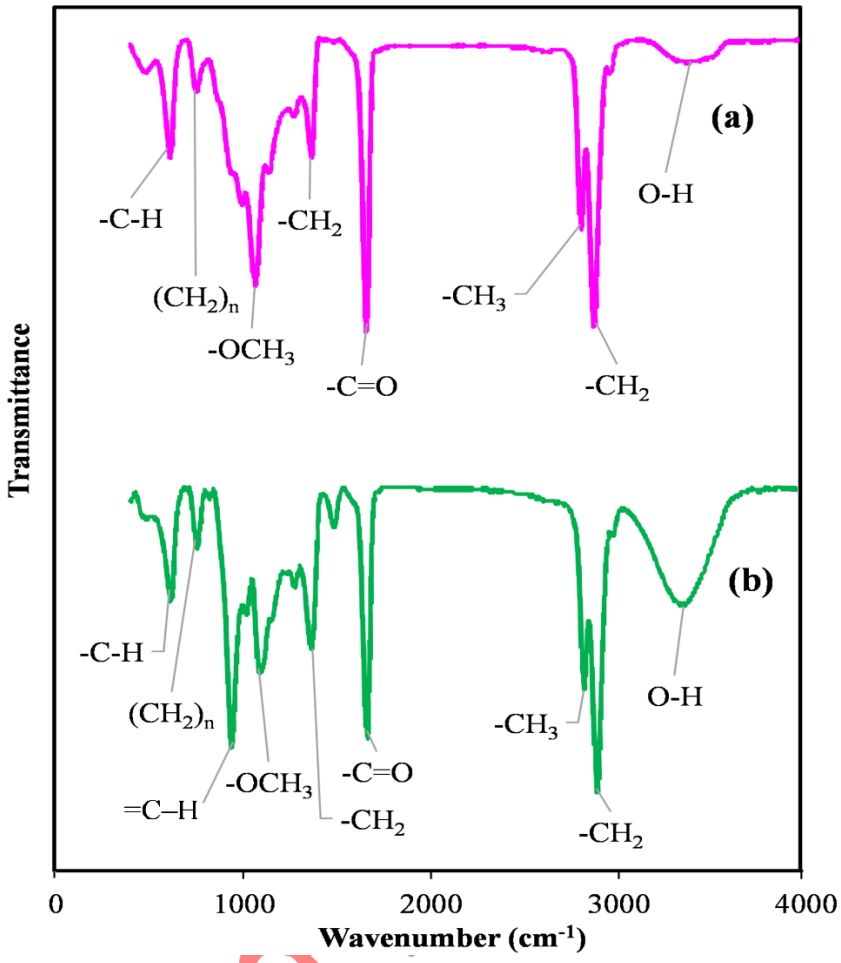

Figure 8. FTIR analysis for identification of functional groups in sunflower oil (a) and biodiesel derived from sunflower oil (b)

3.7 Evaluation of ZnO stability

The stability of heterogeneous catalysts is a key parameter for assessing the economic and operational feasibility of chemical processes, as catalyst stability directly correlates with reduced production costs and enhanced process efficiency [43, 44]. In this study, the stability and recyclability of the zinc oxide nanocatalyst synthesized via the sol-gel method were evaluated over seven consecutive rounds, with outcomes presented in Figure 9. After each reaction round, the catalyst surface was washed with methanol to remove impurities and residues, including methyl

esters and glycerol, and then reused in the subsequent cycle. As shown in Figure 9, biodiesel yield decreased from 89.57% to 80.45% after seven cycles, indicating an approximately 9% reduction in performance. This relatively small decrease demonstrates significant stability of the ZnO nanocatalyst, suggesting that it is a single metal oxide catalyst with a stable structure resistant to chemical degradation [45]. The high catalyst stability is mainly attributed to the strength and durability of the bonds between zinc and oxygen atoms in the nanoparticle structure. Factors contributing to the catalyst activity decline during reuse include blockage of active sites by methyl esters and glycerol, surface poisoning of the catalyst, insufficient washing, and saponification phenomena [45, 46]. Nevertheless, the ZnO nanocatalyst maintained high biodiesel yield after multiple cycles, indicating that it is a suitable, cost-effective option for industrial applications and sustainable biodiesel production.

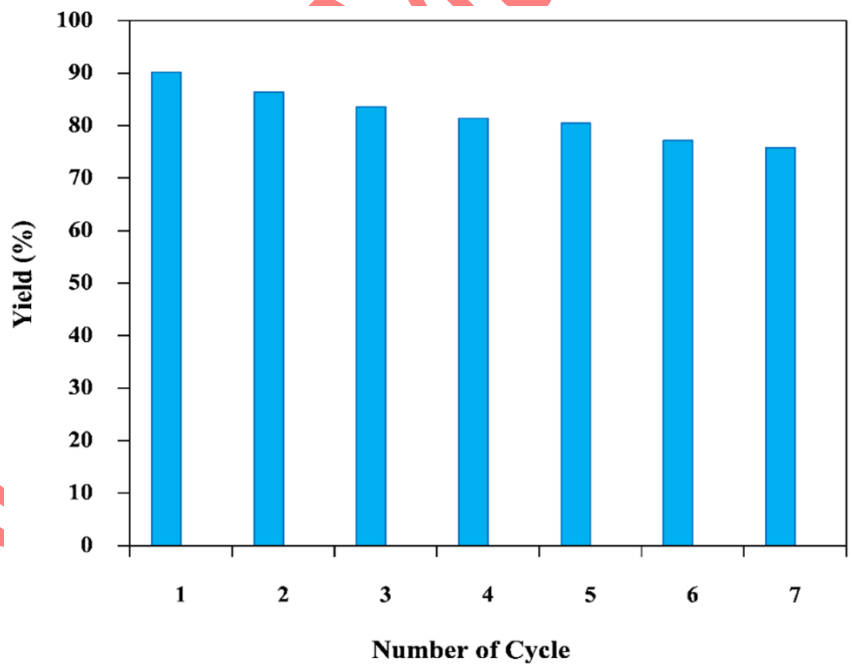

Figure 9. Effect of ZnO nanoparticles reusability on biodiesel yield.

3.8 Evaluation of produced biodiesel characteristics

The physical attributes of methyl ester derived from sunflower oil were measured according to international standards. Kinematic viscosity is an important parameter for diesel engines, significantly influencing the combustion process and fuel injection [50]. Table 5 indicates that the biodiesel's kinematic viscosity was 4.48 cSt, in accordance with ASTM D6751 standards. Additionally, engine injection is highly dependent on fuel density. Higher-density fuel notably reduces the volume of fuel delivered [47]. The measured density of the produced biodiesel was 0.881 g/cm³, also within the standard range. The pour point defines the minimum temperature for fuel pumpability, while the cloud point corresponds to the onset of crystal formation. The flash point is crucial for safe handling and storage [50, 51]. The biodiesel tested showed a pour point of 5 °C and a cloud point of 1 °C, meeting standard limits. The flash point was measured at 169 °C, indicating that sunflower oil-derived biodiesel is safe for storage without special concerns [52]. Another vital biodiesel parameter is the cetane number, indicative of ignition delay. Higher cetane numbers mean better diesel fuel quality [53]. The cetane number of the biodiesel was 52, falling within the standard range. Other properties, such as acid number and water content, were also within acceptable limits. Overall, the physical properties of biodiesel produced from sunflower oil using ZnO nanoparticle catalyst met international ASTM standards, confirming its quality and suitability for use.

Table 5. Comparison of physical properties of biodiesel produced under optimum conditions with ASTM standards.

Feature	ASTM Approach	ASTM Specification	Biodiesel

Specific gravity (g.cm^{-1}@ 15 °C)	D976	0.860-0.900	0.881
Viscosity (cSt @ 40 °C)	D445	2.5-6	4.48
Acid number (mg KOH g-1)	D664	0.5<	0.21
Pour Point (°C)	D97	-15 to +10	-5
Cloud Point (°C)	D2500	-5 to +20	1
Flash Point (°C)	D93	100>	169
Cetane number	D613	47>	52
Water content (ppm)	D95	500<	208

3.9. Comparison of the current research with other previous studies

Table 6 demonstrates that the type of catalyst, oil source, methanol/oil molar proportion, catalyst dosage, and reaction time directly influence biodiesel efficiency. Although previous studies have reported acceptable yields, many required prolonged reaction times (over 120 min) or high catalyst loadings. For instance, the MoO_3/MCM-41 catalyst applied to corn oil at a molar ratio of 20 and a reaction time of 180 min produced an efficiency of only 87.87%, while NiO–CdO–Nd_2O_3 achieved an 80% yield after 300 min. In other cases, such as SnO@γ-Al_2O_3, even with a high catalyst dosage and a large molar ratio (40:1), the yield was as low as 33.5%. In contrast, the present study, utilizing ZnO nanoparticles combined with ultrasonic irradiation, achieved a significantly higher yield (90.5%) in a much shorter reaction time (26.28 min) and with a relatively low catalyst dosage (2.71 wt.%). This clearly highlights the synergistic effect between the high surface area of ZnO nanoparticles and the ability of ultrasonic waves to enhance mass transfer and accelerate reaction kinetics, leading to a remarkable improvement in process efficiency. Therefore, the proposed

method not only demonstrates superior efficiency compared to most previous studies but also provides notable operational benefits in terms of reduced reaction time and catalyst consumption, making it a promising strategy for industrial applications.

Table 6. Comparison of operational reaction parameters with other previous studies.

Catalyst	Feedstock	Molar ratio	Catalyst dosage (wt.%)	Time (min)	Yield (%)	Reference
Cu-ZnO/rGO	olive oil	15.5	10	90	94	[44]
MoO_3/MCM-41	Corn oil	20	3	180	87.87	[45]
NiO–CdO-Nd_2O_3	Mustard oil	15	0.5g	300	80	[46]
Fe_3O_4@ZIF8/TiO_2	Oleic acid	30	6	62.5	80.04	[47]
KNO_3-C/ϒAl_2O_3	Waste cooking oil	18	6	180	88.97	[48]
Fe/SnO	Bitter apple seed oil	10	1	120	98.1	[49]
SrKH/CaO	Canola oil	10	8	60	80	[50]
Fe_3O_4@SiO_2@PIL	Oleic acid	11.5	9.5	240	92	[51]
SnO@ϒ-Al_2O_3	Rapeseed oil	40	10	30	33.5	[52]
ZnO	Sunflower	10.98	2.71	26.28	90.5	This study

3.10. Mechanism of reaction

The mechanism of biodiesel production under ultrasonic irradiation in the presence of ZnO nanoparticles is illustrated in Figure 10. In biodiesel production from sunflower oil, the transesterification reaction involves converting triglycerides into methyl esters (biodiesel) and glycerol using methanol as the alcohol. When ZnO nanoparticles act as a heterogeneous catalyst under ultrasonic conditions, the reaction mechanism is significantly enhanced due to the catalyst's surface properties and ultrasonic energy [4, 12]. ZnO nanoparticles provide a large surface area with active sites such as Zn^{2+} ions, which adsorb methanol. The oxygen ions ($-O^{2-}$) on the ZnO surface deprotonate methanol, generating methoxide ions (CH_3O^-), which serve as strong nucleophiles in the reaction. Simultaneously, triglycerides from sunflower oil adsorb onto the catalyst surface, bringing their ester groups closer to the activated methanol [10, 29]. The methoxide ion attacks the carbonyl carbon of the triglyceride ester bond, forming a tetrahedral intermediate. This intermediate then breaks down, yielding one molecule of methyl ester (biodiesel) and a diglyceride [38, 54]. This process repeats until all triglycerides convert to biodiesel and glycerol. Ultrasound waves induce cavitation effects, enhancing mass transfer and improving contact among ZnO nanoparticles, methanol, and triglycerides [45]. Ultrasonic energy also facilitates methoxide ion formation, stabilizes reaction intermediates, lowers activation energy, and accelerates the reaction under mild conditions. Therefore, combining ZnO nanoparticles with ultrasonic irradiation creates an efficient, recyclable, and eco-friendly method for converting sunflower oil and methanol into biodiesel. This approach increases yield, shortens reaction time, and offers advantages over conventional methods.

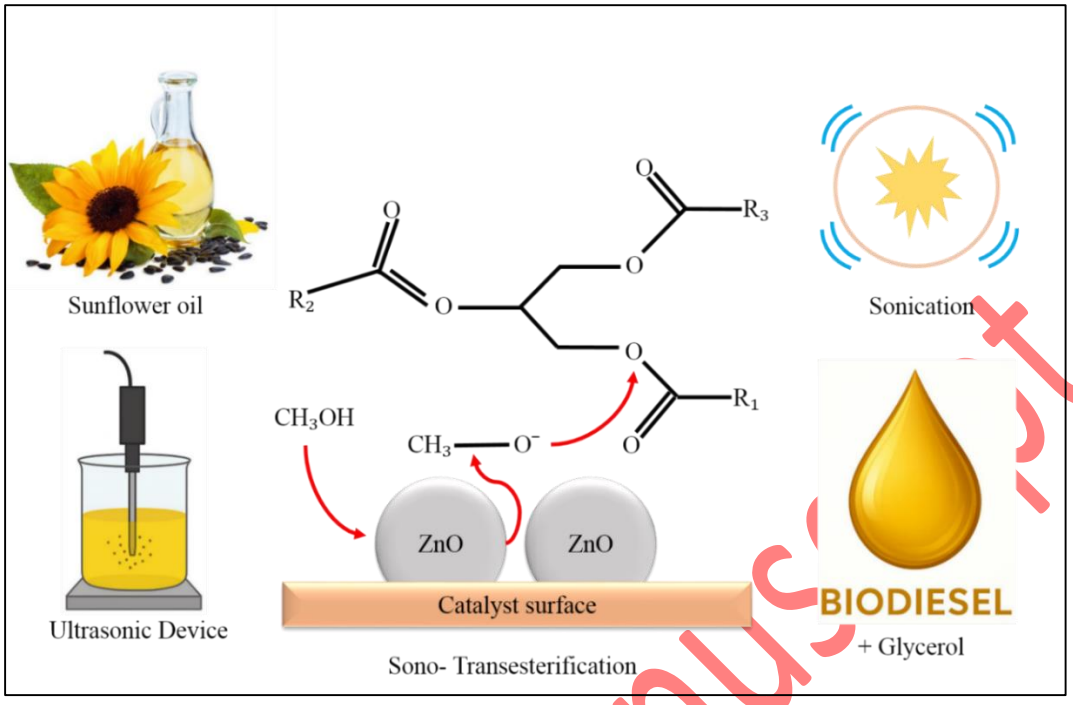

Figure 10. Mechanism of biodiesel generation using ZnO nanoparticles and ultrasound radiation.

4. Conclusion

This study aimed to synthesize ZnO nanocatalysts via the sol-gel approach for the transesterification of sunflower oil under ultrasonic irradiation. The primary goal was to attain the maximum biodiesel efficiency under optimum circumstances and to evaluate the reusability of ZnO nanocatalyst as a single metal oxide nanocatalyst. Three key parameters, the molar proportion of methanol to sunflower oil, sonication time, and nanocatalyst concentration, were selected to investigate their effect on biodiesel yield. RSM-CCD was employed to statistically analyze the effect of reaction variables on biodiesel yield. ANOVA confirmed the robustness of the quadratic models with $R^2 = 0.9969$ and adjusted $R^2 = 0.9939$. The methanol/sunflower oil proportion was identified as the most influential factor. Optimal circumstances included a 10.98:1 molar proportion, 26.28 min sonication, and 2.71 wt.% ZnO dosage. Moreover, the ZnO nanocatalyst

retained acceptable catalytic activity after seven reuse cycles, with more than 80% biodiesel yield maintained, demonstrating excellent catalyst recovery and reusability. Given the high efficiency and reusability of the ZnO nanoparticles in biodiesel production, these nanocatalysts are suitable for the conversion of sunflower oil to methyl ester.

References

[1] M. Ahmad, A.Y. Elnaggar, L.K. Teong, S. Sultana, M. Zafar, M. Munir, E.E. Hussein, S.Z.U. Abidin, Sustainable and eco-friendly synthesis of biodiesel from novel and non-edible seed oil of Monotheca buxifolia using green nano-catalyst of calcium oxide, Energy Convers. Manag.: X 13 (2022) 100142. https://doi.org/10.1016/j.ecmx.2021.100142.

[2] B. Maleki, H. Esmaeili, K.V. Yatish, E, Amruth, Valorization of dairy waste scum oil and rice husk ash-supported CuO nanocatalyst towards cleaner production of biodiesel: A waste-to-energy approach, Process Safety and Environmental Protection. 192 (2024) 1393-1407. https://doi.org/10.1016/j.psep.2024.10.124.

[3] A. Al-Abbasi, F. Almahdi, M. Almaky, R. Izriq, A. Milad, S. Salim, A. Najar, BaO as a heterogeneous nanoparticle catalyst in oil transesterification for the production of FAME fuel, Inorg. Chem. Commun. 158 (2023) 111620. https://doi.org/10.1016/j.inoche.2023.111620.

[4] A.S. Basanagoudar, B. Maleki, M.P. Ravikumar, Mounesh, P. Kuppe, K.V. Yatish, Exploitation of Annona reticulata leaf extract for the synthesis of CeO_2 nanoparticles as catalyst for the production of biodiesel using seed oil thereof, Energy 298 (2024) 131335. https://doi.org/10.1016/j.energy.2024.131335.

[5] R. Foroutan, S.J. Peighambardoust, M. Foroughi, N. S. Peighambardoust, B. Maleki, B. Ramavandi. Recycling the powder of spent alkaline batteries as a sustainable and reusable catalyst in producing biodiesel from waste cooking oil, Environmental Research 271 (2025) 121028. https://doi.org/10.1016/j.envres.2025.121028.

[6] Maleki B, Esmaeili H. Ultrasound-assisted conversion of waste frying oil into biodiesel using Al-doped ZnO nanocatalyst: Box-Behnken design-based optimization. Renewable Energy 2023; 209:10-26. https://doi.org/10.1016/j.renene.2023.03.119.

[7] B. Maleki, S.S. Ashraf Talesh, Sustainable biodiesel production from wild oak (Quercus brantii Lindl) oil as a novel and potential feedstock via highly efficient Co@CuO nanocatalyst: RSM optimization and CI engine assessment, Renew. Energy 224 (2024) 120127. https://doi.org/10.1016/j.renene.2024.120127.

[8] W.N.A. Osman, M.H. Rosli, W.N. Athirah Mazli, Sh. Samsuri, Comparative review of biodiesel production and purification. oil, Renew. Carbon Capture Science & Technology. 13 (2024) 100264. https://doi.org/10.1016/j.ccst.2024.100264.

[9] S. Pandey, I. Narayanan, R. Selvaraj, T. Varadavenkatesan, R. Vinayagam. Biodiesel production from microalgae: A comprehensive review on influential factors, transesterification processes, and challenges, Fuel. 367, (2024), 131547. https://doi.org/10.1016/j.fuel.2024.131547.

[10] A. Rezaeifar, M. Mansouri, B. Maleki, Incorporation of CuO on the αFe_2O_3 nanoparticles as a heterogeneous catalyst for conversion of waste cooking oil into biodiesel, Sci Rep. 15 (2025) 7067. https://doi.org/10.1038/s41598-025-91365-6.

[11] R. Foroutan, S.J. Peighambardoust, R. Mohammadi, S.H. Peighambardoust, B. Ramavandi, Application of walnut shell ash/ZnO/K_2CO_3 as a new composite catalyst for biodiesel generation from Moringa oleifera oil, Fuel 311 (2022) 122624. https://doi.org/10.1016/j.fuel.2021.122624.

[12] S. Tamjidi, B.K. Moghadas, H. Esmaeili, Ultrasound-assisted biodiesel generation from waste edible oil using $CoFe_2O_4$@ GO as a superior and reclaimable nanocatalyst: Optimization of two-step transesterification by RSM, Fuel 327 (2022) 125170. https://doi.org/10.1016/j.fuel.2022.125170.

[13] M. Saberi, S.S. Ashraf Talesh, B. Maleki. Biodiesel production from waste frying oil via $NiFe_2O_4/SiO_2$ magnetic nanocomposites: Evaluation of diesel engine parameters and statistical optimization. Renewable Energy 254 (2025) 123727. https://doi.org/10.1016/j.renene.2025.123727.

[14] T.R. Primadi, F. Fajaroh, A. Santoso, N. Nazriati, E. Ciptawati, Synthesis of CaO@ $CoFe_2O_4$ nanoparticles and its application as a catalyst for biodiesel production from used cooking oil, Key Eng. Mater. 851 (2020) 184-193. https://doi.org/10.4028/www.scientific.net/KEM.851.184.

[15] R.A. Omar. Mawlid [1], Hosam H. Abdelhady [1], Mohamed S. El-Deab, Highly active novel K_2CO_3 supported on $MgFe_2O_4$ magnetic nanocatalyst for low-temperature conversion of waste cooking oil to biodiesel: RSM optimization, kinetic, and thermodynamic studies, Journal of Environmental Chemical Engineering. 11, (2023), 110623. https://doi.org/10.1016/j.jece.2023.110623.

[16] Y. Rajput, P. Kumar, T.C. Zhang, D. Kumar, M. Nemiwal, Recent advances in g-C3N4-based photocatalysts for hydrogen evolution reactions, Int. J. Hydrogen Energy 47 (2022) 38533-38555. https://doi.org/10.1016/j.ijhydene.2022.09.038.

[17] M. Stefan, C. Leostean, A. Popa, D. Toloman, I. Perhaita, A. Cadis, S. Macavei, O. Pana, Highly stable MWCNT-$CoFe_2O_4$ photocatalyst. EGA-FTIR coupling as efficient tool to illustrate the formation mechanism, J. Alloys Compd. 928 (2022) 167188. https://doi.org/10.1016/j.jallcom.2022.167188.

[18] S. Mishra, L. Acharya, S. Sharmila, K. Sanjay, R. Acharya. Designing g-C3N4/NiFe2O4 S-scheme heterojunctions for efficient photocatalytic degradation of Rhodamine B and tetracycline hydrochloride, Appl. Surf. Sci. Adv. 24 (2024) 100647. https://doi.org/10.1016/j.apsadv.2024.100647.

[19] H. A. El-Sabban, A.H. Mady, M.A. Diab, S.Y. Attia, S.G. Mohamed, Construction of novel dual Z-scheme heterojunction of ternary CdS/g-C3N4/NiFe2O4 magnetically retrievable nanocomposite for boosted photocatalytic and energy storage applications, Surf. Interfaces 44 (2024) 103798. https://doi.org/10.1016/j.surfin.2023.103798.

[20] X. Liu, Q. Wang, P. Shu, Y. Wu, X. Li, J. Luo, Multicomponent competitive synergistically active $NiFe_2O_4$/C-g-C_3N_4/RGO heterostructure for efficient electromagnetic wave absorption, Carbon 234 (2025) 119964. https://doi.org/10.1016/j.carbon.2024.119964.

[21] W. Muhammad, W. Ali, M. Asif Khan, F. Ali, A. Zada, M.Z. Ansar, P.S. Yap, Construction of visible-light-driven 2D/2D $NiFe_2O_4$/g-C_3N_4 Z-scheme heterojunction photocatalyst for effective degradation of organic pollutants and CO_2 reduction, J. Environ. Chem. Eng. 12 (2024) 113409. https://doi.org/10.1016/j.jece.2024.113409.

[22] Li X, Zhu J, Niu S, Zheng Y, Xu Y. Novel acid-base dual-activity heterogeneous Ba40-Ce15/ZSM-5 catalyst for biodiesel production: RSM-based optimization and performance analysis. Energy 2025; 333:137451. https://doi.org/10.1016/j.energy.2025.137451.

[23] Yaakouby I El, Borji A, Ettalibi O, Kouar J, Abouliatim Y, Hlaibi M, et al. One-pot conversion Allium sativum peels into a cost-effective carbon-based heterogeneous acid catalyst for renewable biodiesel production using palm oil refining by-products. Energy Conversion and Management 2025; 327:119551. https://doi.org/10.1016/j.enconman.2025.119551.

[24] R. Karami, M.G. Rasul, M.M.K. Khan, M.M. Salahi, M. Anwar, Experimental and computational analysis of combustion characteristics of a diesel engine fueled with diesel-tomato seed oil biodiesel blends, Fuel 285 (2021) 119243. https://doi.org/10.1016/j.fuel.2020.119243.

[25] B. Maleki, Y.K. Venkatesh, B. Muthusamy, H. Esmaeili, A cleaner approach towards magnetically assisted-electrolysis of biodiesel production using novel $MnFe_2O_4$@ sawdust derived biochar nanocatalyst and its performance on a CI engine, Energy Convers. Manag. 299 (2024) 117829. https://doi.org/10.1016/j.enconman.2023.117829.

[26] B. Maleki, Y.K. Venkatesh, S.S.A. Talesh, H. Esmaeili, S. Mohan, G.R. Balakrishna, A novel biomass derived activated carbon mediated AC@ ZnO/NiO bifunctional nanocatalyst to produce high-quality biodiesel from dairy industry waste oil: CI engine performance and emission, Chem. Eng. J. 467 (2023) 143399. https://doi.org/10.1016/j.cej.2023.143399.

[27] S. Ilmi, M. Sabri, E.F. Ginting, J.J Silalahi, Biodiesel production of WCO-neem oil and mixed using pilot plant scale with ultrasound and overhead stirred and characteristic of emissions in fire tube boiler, Case Stud. Chem. Environ. Eng. 11 (2025) 101029. https://doi.org/10.1016/j.cscee.2024.101029.

[28] C. Wang, H. Xia, Y. Xu, Z. Lu, Q. Pei, L. Dai, L. Zhang, Efficient recovery of valuable metals from low-grade zinc residue by ultrasonic strengthening, Chem. Eng. Process.: Process Intensif. 211 (2025) 110240. https://doi.org/10.1016/j.cep.2025.110240.

[29] B. Maleki, S.Siamak Ashraf Talesh, Optimization of ZnO incorporation to αFe_2O_3 nanoparticles as an efficient catalyst for biodiesel production in a sonoreactor: application on the CI engine. Renewable Energy, 2022. 182: p. 43-59. https://doi.org/10.1016/j.renene.2021.10.013.

[30] A.K. Prajapati, S.S. Ali, K.B. Ansari, M. Athar, M.K. Al Mesfer, M. Shah, M. Danish, R. Kumar, S. Raheman. Process intensification in biodiesel production using unconventional reactors, Fuel 380 (2025) 133263. https://doi.org/10.1016/j.fuel.2024.133263.

[31] R.M. Ali, E. Salama, H.A. Hamad. A novel technology for microwave-assisted synthesis of new Ca/Si/Al composite oxide-based catalyst for boosting the ultrasound-assisted biodiesel production, Process Saf. Environ. Prot. 194 (2025) 674-687. https://doi.org/10.1016/j.psep.2024.12.042.

[32] Maleki B, Ashraf Talesh SS. Pour point and yield simultaneous improvement of alkyl esters produced by ultrasound-assisted in the presence of αFe_2O_3/ZnO: RSM approach. Fuel 2021; 298:120827. https://doi.org/10.1016/j.fuel.2021.120827.

[33] Sun H, Ma M, Fan M, Sun K, Xu W, Wang K, et al. Controllable preparation of biomass derived mesoporous activated carbon supported nano-CaO catalysts for biodiesel production. Energy 2022; 261:125369. https://doi.org/10.1016/j.energy.2022.125369.

[34] B. Gurunathan, A. Ravi, Biodiesel production from waste cooking oil using copper doped zinc oxide nanocomposite as heterogeneous catalyst, Bioresour. Technol. 188 (2015) 124-127. https://doi.org/10.1016/j.biortech.2015.01.012.

[35] Y. Man, M. Habibi, B. Maleki. Biodiesel synthesis from waste coconut scum oil utilizing $SnFe_2O_4$/cigarette butt-derived biochar as a magnetic nanocatalyst: Optimization, kinetic and

thermodynamic study. Chemical Engineering Research and Design 210 (2024) 311–327. https://doi.org/10.1016/j.cherd.2024.08.033.

[36] X. Yang, W. Liu, R. Zhao, A. Raise, Enhanced conversion of non-edible Jatropha oil to biodiesel utilizing highly reusable Mg decorated $CoFe_2O_4$ nanocatalyst: Optimization by RSM, Ind. Crops Prod. 204 (2023) 117319. https://doi.org/10.1016/j.indcrop.2023.117319.

[37] M.R. Elamin, N.Y. Elamin, A.H. Alluhayb, K.K. Taha, M.A. Ben Aissa, A. Mallah, A. Modwi, Efficient NiFe2O4@ g-C3N4 Nanosorbent for Oxytetracycline Adsorption: Removal Modeling and Selectivity, J. Electron. Mater. 53 (10) (2024) 6164-6180. https://doi.org/10.1007/s11664-024-11216-4.

[38] B. Maleki, K.V. Yatish, H. Esmaeili, M. Haddadi, R.M. Prakash, G.R. Balakrishna, Novel Co_3O_4 decorated with rGO nanocatalyst to boost microwave-assisted biodiesel production and as nano-additive to enhance the performance-emission characteristics of diesel engine, Energy 289 (2024) 129944. https://doi.org/10.1016/j.energy.2023.129944.

[39] B. Maleki, B. Singh, H. Esmaeili, K.V. Yatish, S.S. Ashraf Talesh, S. Seetharaman, Transesterification of waste cooking oil to biodiesel by walnut shell/sawdust as a novel, low-cost and green heterogeneous catalyst: Optimization via RSM and ANN, Ind. Crops Prod. 193 (2023) 116261. https://doi.org/10.1016/j.indcrop.2023.116261.

[40] A. Sharma, P. Kodgire, S.S. Kachhwaha, Investigation of ultrasound-assisted KOH and CaO catalyzed transesterification for biodiesel production from waste cotton-seed cooking oil: Process optimization and conversion rate evaluation, J. Clean. Prod. 259 (2020) 120982. https://doi.org/10.1016/j.jclepro.2020.120982.

[41] N. Prajapati, S.S. Kachhwaha, P. Kodgire, R.K. Vij, A novel high-speed homogenizer assisted process intensification technique for biodiesel production using soya acid oil: Process optimization, kinetic and thermodynamic modelling, Energy Convers. Manag. 324 (2025) 119302. https://doi.org/10.1016/j.enconman.2024.119302.

[42] Q. Li, Y. Zhao, T. Liu, Z. Luo, K. Luo, T. Wang, Kinetic and optimization study of ultrasound-assisted biodiesel production from waste coconut scum oil using porous $CoFe_2O_4$@sulfonated graphene oxide magnetic nanocatalysts: CI engine approach, Renew. Energy 236 (2024) 121457. https://doi.org/10.1016/j.renene.2024.121457.

[43] M.A. Abo El-Khair, Mo.El saied, A.O. Abo El Naga, A.S. Morshedy, Rapid and low-temperature biodiesel production from waste cooking oil: Kinetic and thermodynamic insights using a KOH/$ZnAl_2O_4$ nanocatalyst derived from waste aluminum foil, Energy Convers. Manag. 318 (2024) 118898. https://doi.org/10.1016/j.enconman.2024.118898.

[44] S. Hasannia, M. Kazemeini, M. Tamtaji, M. Mirzaeian, An environmentally friendly biodiesel Production: Computational and experimental investigations of ZnO-based catalysts for enhanced olive oil conversion, Renewable Energy, 2025, 251, 123393. https://doi.org/10.1016/j.renene.2025.123393.

[45] J. C. F. Cavalcante, A. M. da Silva, P. M. B. Caldas, B. V. de Sousa Barbosa, H. B. da Silva Junior and J. J. N. Alves, ´ Characterization and optimization of biodiesel production from corn oil using heterogeneous MoO_3/ MCM-41 catalysts, Catal. Today, 2025, 446, 115119. https://doi.org/10.1016/j.cattod.2024.115119.

[46] M. Zeeshan, S. Ghazanfar, M. Tariq, H. M. Asif, A. Hussain, M. Usman, M. A. Khan, K. Mahmood, M. Sirajuddin and M. Imran, Synthesis of novel ternary NiO-CdO-Nd_2O_3

nanocomposite for biodiesel production, Renewable Energy, 2023, 210, 800–809. https://doi.org/10.1016/j.renene.2023.04.077.

[47] A. M. Sabzevar, M. Ghahramaninezhad and M. N. Shahrak, Enhanced biodiesel production from oleic acid using TiO_2- decorated magnetic ZIF-8 nanocomposite catalyst and its utilization for used frying oil conversion to valuable product, Fuel, 2021, 288, 119586. https://doi.org/10.1016/j.fuel.2020.119586.

[48] J. Suresh, H. S. Yong, N. B. Talib, J. Matmin, N. I. W. Azelee, S. J. M. Rosid and S. Toemen, Biomass-incorporated KNO_3- C/g-Al_2O_3 bifunctional catalyst for efficient biodiesel production, Renewable Energy, 2024, 234, 121239. https://doi.org/10.1016/j.renene.2024.121239.

[49] M. Hanif, I. A. Bhatti, M. Zahid and M. Shahid, Production of biodiesel from non-edible feedstocks using environment friendly nano-magnetic Fe/SnO catalyst, Sci. Rep., 2022, 12, 16705. https://doi.org/10.1038/s41598-022-20856-7.

[50] M.A. Hernandez-Martínez, ´ J.A. Rodriguez, G. Chavez-Esquivel, D. Angeles-Beltr ´ ´ an, J.A. Tavizon-Pozos, ´ Canola oil transesterification for biodiesel production using potassium and strontium supported on calcium oxide catalysts synthesized from oyster shell residues, Next Mater. 1 (2023) 100033. https://doi.org/10.1016/j.nxmate.2023.100033.

[51] J. Ding, C. Zhou, Z. Wu, C. Chen, N. Feng, L. Wang, H. Wan and G. Guan, Core-shell magnetic nanomaterial grafted spongy-structured poly (ionic liquid): A recyclable brönsted acid catalyst for biodiesel production, Appl. Catal., A, 2021, 616, 118080. https://doi.org/10.1016/j.apcata.2021.118080.

[52] C. Prestigiacomo, M. Biondo, A. Galia, E. Monflier, A. Ponchel, D. Prevost, O. Scialdone, S. Tilloy and R. Bleta, Interesterification of triglycerides with methyl acetate for biodiesel production using a cyclodextrinderived SnO@g-Al_2O_3 composite as heterogeneous catalyst, Fuel, 2022, 321, 124026. https://doi.org/10.1016/j.fuel.2022.124026.

[53] Wang, X.M., Zeng, Y.N., Jiang, L.Q., Wang, Y.T., Li, J.G., Kang, L.L., Ji, R., Gao, D., Wang, F.P., Yu, Q., Wang, Y.J., 2022. Highly stable $NaFeO_2$-Fe_3O_4 composite catalyst from blast furnace dust for efficient production of biodiesel at low temperature. Ind. Crops Prod. 182, 114937. https://doi.org/10.1016/j.indcrop.2022.114937.

[54] Maleki B, Esmaeili H, Mansouri M, Kumar D, Singh B. Enhanced conversion of dairy waste oil to biodiesel via novel and highly reactive UiO-66-NH_2/ZnO/TiO_2 nano-catalyst: Optimization, kinetic, thermodynamic and diesel engine studies. Fuel 2022; 340:126901. https://doi.org/10.1016/j.fuel.2022.126901.